Dielectric and Raman studies of $(Ba_xPb_{1-x})(Yb_{0.5}Nb_{0.5})O_3$

2005 J. Phys.: Condens. Matter 17 361

(http://iopscience.iop.org/0953-8984/17/2/011)

INSTITUTE OF PHYSICS PUBLISHING JOURNAL OF PHYSICS: CONDENSED MATTER

J. Phys.: Condens. Matter **17** (2005) 361–372 doi:10.1088/0953-8984/17/2/011

Dielectric and Raman studies of $(Ba_xPb_{1-x})(Yb_{0.5}Nb_{0.5})O_3$

R R Vedantam[1], **V Subramanian**[1,3], **V Sivasubramanian**[2] **and V R K Murthy**[1]

[1] Microwave Laboratory, Department of Physics, Indian Institute of Technology, Chennai-600 036, India
[2] Materials Science Division, Indira Gandhi Centre for Atomic Research, Kalpakkam-603 102, India

E-mail: manianvs@iitm.ac.in (V Subramanian)

Received 29 July 2004, in final form 26 November 2004
Published 20 December 2004
Online at stacks.iop.org/JPhysCM/17/361

Abstract

Dielectric dispersion and Raman studies are carried out on the solid solution series $(Ba_xPb_{1-x})(Yb_{0.5}Nb_{0.5})O_3$ from $x = 0.0$ to 0.3. The x-ray diffraction analysis indicates that with the substitution of Ba^{2+}, the intensity of the peaks corresponding to antiparallel displacement of Pb^{2+} decreases and the structure becomes cubic. The low frequency dielectric dispersion studies indicate that the series undergoes a transition from an antiferroelectric to a relaxor ferroelectric with variation of x. Raman spectra of the compositions indicate the presence of a greater number of modes for the compounds with cubic structure ($x \geqslant 0.2$). A new mode at 420 cm^{-1} is observed for the compounds with Ba^{2+} substitution. The intensity of this mode increases monotonically with increase in Ba^{2+} substitution and this has been attributed to the commencement of local distortion. This could be responsible for the appearance and increase in the diffuseness around T_{max}, the temperature corresponding to $\varepsilon'_{r,max}$.

1. Introduction

Lead based complex perovskites attract wide academic interest owing to their numerous applications and the physical properties that they exhibit. The physical properties exhibited by these compounds depend on the B-site ordering [1–4]. The compounds with general formula $Pb(B'_xB''_{1-x})O_3$ can be divided into two categories, namely $Pb(B'_{1/3}B''_{2/3})O_3$ and $Pb(B'_{1/2}B''_{1/2})O_3$. The compounds with $x = 1/3$ usually exhibit short range 1:1 B-site ordering [5, 6]. The compounds with $x = 0.5$ exhibit (a) complete B-site ordering [7, 8], (b) no ordering in the B-site [9] and (c) B-site ordering that can be varied by using different thermal treatments [3, 4]. In compounds with long range ordering in the B-site, the transition

[3] Author to whom any correspondence should be addressed.

is sharp (the temperature of the transition is well defined) and in the x-ray diffraction (XRD) pattern for these compounds distinct superlattice reflections are observed corresponding to B-site ordering [7, 8].

Lead ytterbium niobate, $Pb(Yb_{0.5}Nb_{0.5})O_3$ (PYN), belongs to the $Pb(B'_{1/2}B''_{1/2})O_3$ group of lead based complex perovskites with highly ordered B-site cations. PYN undergoes a phase transition from the paraelectric cubic to the antiferroelectric orthorhombic phase at 583 K [7]. Above T_c, the cubic structure has the space group $Fm3m$ corresponding to 1:1 ordering of B-site ions. Below T_c, in addition to B-site ordering, there is antiparallel displacement of Pb^{2+} ions that results in orthorhombic structure with the space group $Pnam$. Reflections corresponding to antiparallel displacement of lead cations and F reflections corresponding to B-site ordering are observed in the room temperature XRD pattern [7]. The structural phase transition in PYN is very sharp and the temperatures T_{max} and T'_{max} corresponding to $\varepsilon'_{r,max}$ and $\varepsilon''_{r,max}$ respectively are not frequency dependent.

Substitution of Ba^{2+} for Pb^{2+} in PYN results in interesting changes in the dielectric properties [10–12]. Choo and Kim [10] observed that with increase in the Ba^{2+} substitution the dielectric response changes from that of an antiferroelectric to that of a relaxor ferroelectric. They observed that the dielectric response becomes increasingly diffuse with increase in Ba^{2+} concentration and a pure diffuse phase transition is observed for $x \geqslant 0.15$. They attribute the diffuseness to the presence of polar clusters with local structure distortions within a non-polar matrix.

Raman scattering is the appropriate technique for getting more insight into the local distortions present in these systems. Studies on Raman active optical phonon modes have been reported for many lead based complex perovskites. The relaxor ferroelectric $Pb(Mg_{1/3}Nb_{2/3})O_3$ (PMN) exhibits complex Raman spectra though the macroscopic structure has cubic symmetry. Raman spectra of PMN have been interpreted in terms of the existence of 1:1 ordered nanoclusters and of local structural distortion whose symmetry is lower than cubic [13, 14]. Recently Jiang *et al* [15] and Kim [16] reported Raman studies on nanoscale 1:1 B-site ordering in PMN with partial substitution of Na^+, Bi^{3+} and La^{3+} for Pb^{2+}. They obtained the degree of B-site ordering from the full width at half-maximum (FWHM) of Raman modes corresponding to 1:1 ordering. The changes in the degree of ordering for the quenched and annealed $Pb(Sc_{0.5}Ta_{0.5})O_3$ [17, 18] have been reported from Raman spectra studies. Recently Mihailova *et al* [19] assigned the symmetry of Raman modes for disordered $Pb(Sc_{0.5}Nb_{0.5})O_3$ (PSN) and $Pb(Sc_{0.5}Ta_{0.5})O_3$ (PST) on the basis of normal mode calculations.

In the present study, x-ray diffraction, dielectric and Raman spectra studies were carried out on the solid solution series $(Ba_xPb_{1-x})(Yb_{0.5}Nb_{0.5})O_3$ for $x = 0$, 0.05, 0.1, 0.15, 0.2, 0.25 and 0.3. As the solid solution series exhibits a crossover from antiferroelectric to relaxor behaviour for $x \geqslant 0.15$, it is important to understand the behaviour of Raman active phonon modes in the above-mentioned solid solution system. The changes in the Raman spectra are discussed in relation to a conjecture regarding the structural and dielectric susceptibility on substitution of Ba^{2+} for Pb^{2+}.

2. Experimental details

The conventional solid state reaction route is followed for the preparation of the compositions $(Ba_xPb_{1-x})(Yb_{0.5}Nb_{0.5})O_3$ for $x = 0$, 0.05, 0.1, 0.15, 0.2, 0.25 and 0.3. Apart from PYN, the compositions are prepared using a single-step process since addition of Ba^{2+} stabilizes the perovskite phase avoiding the formation of secondary phase. The high purity reagents PbO, $BaCO_3$, Yb_2O_3 and Nb_2O_5 are taken in the stoichiometric ratio and calcined. The powders are calcined between 900 and 1000 °C. The calcined powders are reground and pellets are made.

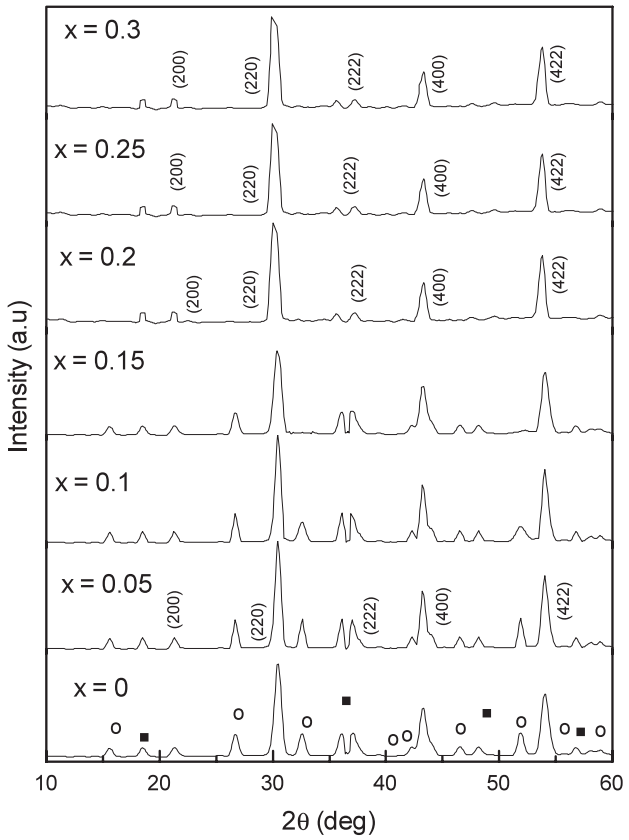

Figure 1. X-ray diffraction patterns of the compositions at room temperature; O, the superlattice reflection corresponding to antiparallel displacement of Pb^{2+} cations and, ■, the F reflection due to B-site ordering.

The pellets are sintered between 1100 and 1300 °C. Two-step solid state reaction is used to synthesize PYN to avoid the formation of secondary phases. Initially Yb_2O_3 and Nb_2O_5 are taken in the stoichiometric ratio, mixed with distilled water as the medium and calcined at 1300 °C for 24 h to form $YbNbO_4$. $YbNbO_4$ and PbO are taken in the stoichiometric ratio and calcined at 900 °C for 2 h. Sintering is carried out at 1100 °C for 2 h. Phase confirmation is carried out using XRD. The temperature variation of the low frequency dielectric response is carried out using a Zentech-1061 LCZ meter.

Sintered pellets were used for recording Raman spectra at room temperature. The pellets were polished on one side using 0.25 μm diamond paste and subsequently annealed at 500 °C for 8 h to remove the residual surface stress left from polishing. Raman spectra were recorded in the back-scattering geometry using 200 mW of power of a 488 nm line from an Ar-ion laser. The scattered light was analysed using a double monochromator (SPEX 14018) and detected using a photomultiplier tube (FW ITT130) operating in the photon counting mode. The position, intensity and linewidth (FWHM) of the Raman spectra were obtained using the Jandel peak fit program. The Lorentzian line shape was used to describe the peak shapes in the spectrum.

3. Results and discussion

Figure 1 shows the XRD pattern for the compositions. The single phase is confirmed from the XRD studies at room temperature. No additional peaks corresponding to secondary phase

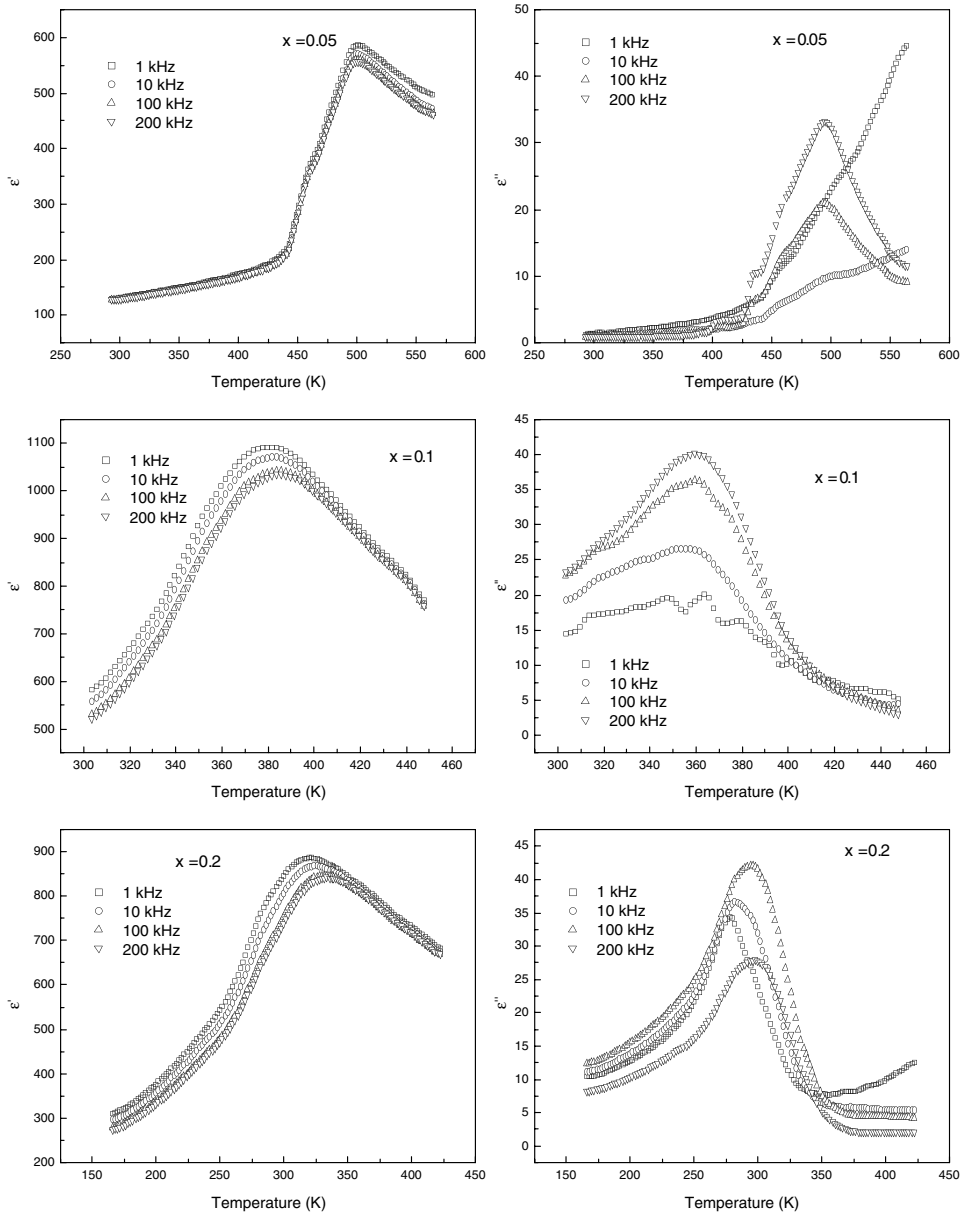

Figure 2. The temperature dependence of ε_r' and ε_r'' for the compositions with $x = 0.05$, $x = 0.1$ and $x = 0.2$.

are observed. For pure PYN, reflections corresponding to B-site ordering and antiparallel displacement of Pb^{2+} were observed. With increase in the Ba^{2+} concentration, the intensity of the reflections corresponding to the B-site ordering at $2\theta = 18.6°$ and $37.2°$ does not change very much. However, the peaks corresponding to antiparallel displacement of Pb^{2+} become weak and disappear completely for $x \geqslant 0.15$.

Figure 2 shows the dielectric response for some of the compositions studied. The phase transition is very sharp and is independent of frequency for PYN. For $x \geqslant 0.1$ the phase

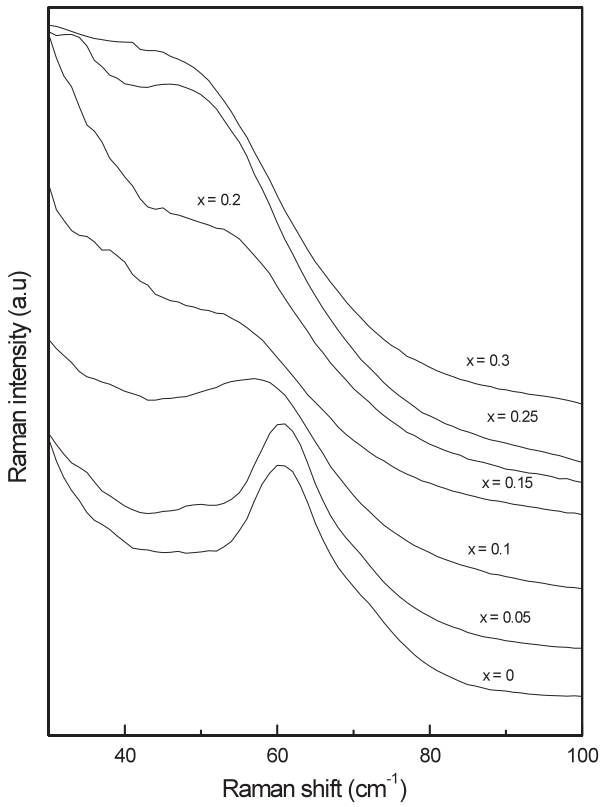

Figure 3. Raman spectra in the frequency region below 100 cm^{-1}.

transition becomes more diffuse. For compositions $x \geqslant 0.1$, the temperatures T_{max} and T'_{max} corresponding to $\varepsilon'_{r,max}$ and $\varepsilon''_{r,max}$ respectively become frequency dependent. Both T_{max} and T'_{max} gradually decrease with increase in Ba^{2+} substitution, as can be observed from figure 2. The response of the three compositions is only given where subtle changes were observed.

The entire frequency range of the Raman spectra is plotted in three figures for convenience. The spectra of all the compositions for the frequency region below 100 cm^{-1} are given in figure 3. The results for the region between 100 and 400 cm^{-1} and that between 400 and 1000 cm^{-1} are given in figures 4 and 5 respectively. The corresponding positions and linewidths of the modes are tabulated in tables 1, 2 for clarity.

The symmetry of the antiferroelectric and paraelectric phases of PYN is same as that for Pb_2MgWO_6 (PMW) [20, 21]. The group theoretical analysis [22] predicts 60 Raman active modes in the antiferroelectric orthorhombic phase:

$$\Gamma_{Raman} = 18A_g + 18B_{1g} + 12B_{2g} + 12B_{3g}$$

and four Raman active modes in the paraelectric cubic phase:

$$\Gamma_{Raman} = A_{1g} + E_g + 2F_{2g}.$$

In the present case it is observed that, in the orthorhombic phase, the number of modes is less than 60. This could be due to merging of closely spaced modes because of thermal broadening, low polarizability and degeneracy of certain modes. For PMW, 40 modes at 10 K have been reported [23]. In the present study, with increase in the Ba^{2+}, the structure becomes cubic,

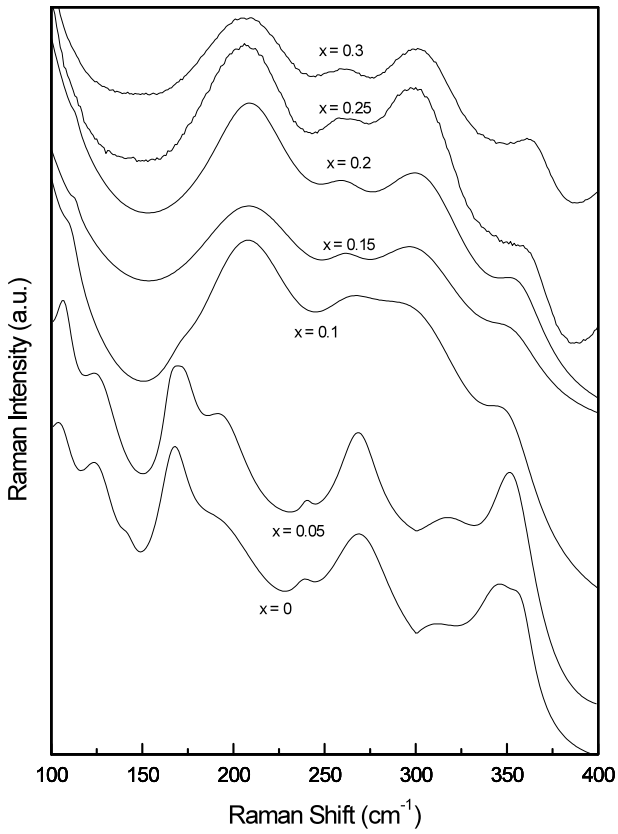

Figure 4. Raman spectra in the frequency range 100–400 cm^{-1}.

as is evident from the XRD. For this cubic phase, the number of modes observed is more than predicted by group theory analysis, as in the case of PSN and PST. Therefore for the compositions in the present study, it is not possible to assign the symmetry of the modes on the basis of group theoretical analysis alone. Hence, we have followed the work of Mihailova *et al* [19] for the assignment of the symmetry of modes. For the complete description of the modes of PSN and PST, they took into account the effect of local structural distortion and electron–phonon coupling in their model calculation in addition to the modes possible for cubic symmetry with space group $Fm3m$.

Two triply degenerate F_{2g} phonon modes are observed at 55 and 520 cm^{-1}. These two modes are expected to split into three lines as the symmetry reduces to orthorhombic. However, in the present case the splitting is not prominently seen for both modes, as was observed for PMW, PST and PSN [19, 22]. However, for PYN and for the compound with $x = 0.05$, a faint shoulder near 70 cm^{-1} can be seen. For the compositions beyond $x = 0.05$, the splitting could not be observed. The mode at 55 cm^{-1} corresponds to Pb–O stretching. The mode is influenced by the mass of A-site cations and the A–O binding force. Hence the corresponding mode occurs in the low frequency region. For many lead based complex perovskites, this mode is observed in the range 50–60 cm^{-1} [19, 22]. It is expected that the frequency of this mode should increase with increase in Ba^{2+} content, as the mass of Ba (137.3) is less than that of Pb (207.2). With increase in Ba^{2+} content, the frequency of this mode decreases to 50 cm^{-1} and

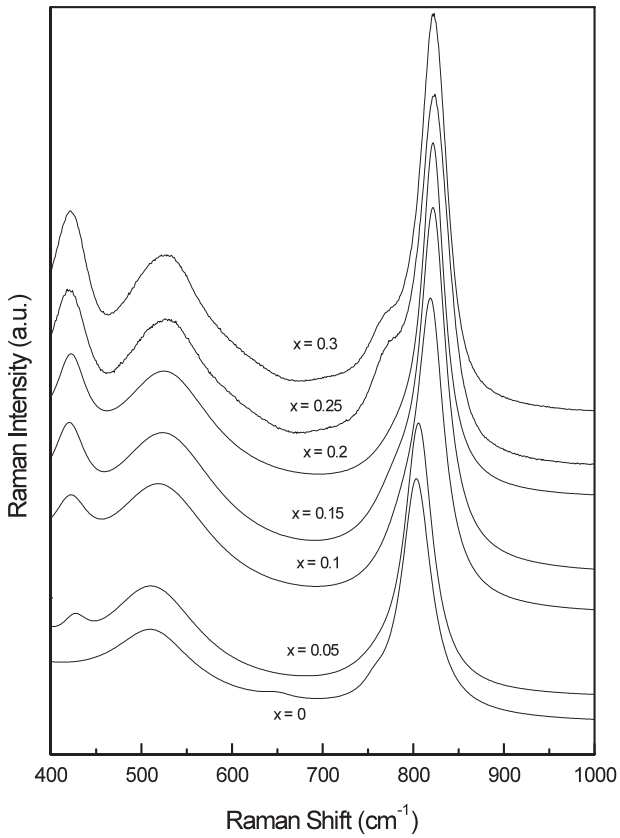

Figure 5. Raman spectra in the frequency range 400–1000 cm^{-1}.

the FWHM increases to 17 cm^{-1}. This indicates considerable softening of the force constant of the corresponding vibration. The broadening observed with increase in Ba^{2+} may be due to the disordered distribution of Ba^{2+} ions. The mode at 520 cm^{-1} due to symmetric O–B–O bending shows an increase in intensity with increase in substitution of Ba^{2+}, as can be seen from figure 5. The FWHM does not exhibit any uniform variation.

The intensity of the modes at 105 and 167 cm^{-1} decreases monotonically and vanishes at $x = 0.20$. Interestingly, this corresponds to the disappearance of the diffraction peaks associated with the antiparallel displacement of Pb^{2+} ions beyond $x = 0.15$. In the absence of detailed lattice calculations, quantitative assignment of these modes is not possible but they may be assignable to orthorhombic distortion due to Pb^{2+} ions.

The presence of ions of different valence and ionic size in the B-site results in the relative rotation of the octahedron due to size mismatch in the B′–O–B″ bond. This gives rise to an F_{1g} mode around 200 cm^{-1}. With increase in Ba^{2+} content, the frequency of the mode changes marginally. The intensity of this mode increases with increase in the Ba^{2+} concentration.

Two of the four F_{1u} phonon modes observed at 265 and 420 cm^{-1} are sensitive to the mass and symmetry of B-site ions. The mode at 265 cm^{-1} corresponds to localization of B-site cations. The frequency of this mode decreases slightly whereas the intensity decreases drastically with increase in the Ba^{2+} content.

Two F_{2u} modes at 303 and 353 cm^{-1} arise due to electron–phonon coupling of Pb^{2+} lone pair electrons [24, 25]. The frequency and the FWHM of these two modes do not show

Table 1. The frequency (ω) and linewidth (Γ) of the modes due to cubic and lower local symmetry.

Composition	F_{2g}		F_{1g}		F_{1u}		F_{2u}				F_{1u}		F_{2g}		E_g		A_{1g}	
x	ω (cm^{-1})	Γ (cm^{-1})	ω (cm^{-1})	Γ (cm^{-1})	ω (cm^{-1})	Γ (cm^{-1})	ω (cm^{-1})	Γ (cm^{-1})	ω (cm^{-1})	Γ (cm^{-1})	ω (cm^{-1})	Γ (cm^{-1})	ω (cm^{-1})	Γ (cm^{-1})	ω (cm^{-1})	Γ (cm^{-1})	ω (cm^{-1})	Γ (cm^{-1})
0.00	61	6	192	30	270	22	303	42	345	16	—	—	512	53	757	14	803	20
0.05	61	6	194	17	269	14	318	41	353	16	426	18	511	65	766	35	806	18
0.10	59	10	207	40	263	27	302	44	351	18	422	25	520	71	791	32	819	17
0.15	55	15	208	44	261	22	301	38	353	19	420	23	525	74	783	35	822	17
0.20	55	13	209	43	261	16	303	38	357	17	422	21	526	65	789	36	821	14
0.25	50	17	206	38	260	17	301	33	358	12	421	21	528	70	774	33	823	18
0.30	52	15	206	39	260	16	303	30	361	10	421	21	528	65	772	37	822	16
	Pb–O stretching		BO_3 rotation		B localized		Pb^{2+} e^-–phonon coupling				O–B–O asymmetric bending (ferroic)		O–B–O symmetric bending		B–O symmetric stretching		B′–O–B″ symmetric stretching	

Table 2. The frequency (ω) and linewidth (Γ) of the modes due to orthorhombic symmetry.

Composition x	ω (cm^{-1})	Γ (cm^{-1})	Corresponding mode of vibration
0.00	105	9	
0.05	107	6	
0.10	111	5	
0.15	113	2	Orthorhombic distortion
0.20	—	—	
0.25	—	—	
0.30	—	—	
0.00	142	5	
	167	10	
0.05	165	6	
	172	9	
0.10	170	10	Orthorhombic distortion
0.15	—	—	
0.20	—	—	
0.25	—	—	
0.30	—	—	

significant variation with increase in Ba^{2+} substitution. The F_{2u} mode consists of O vibrations along the Pb–O bonds, i.e. it appears as a Pb–O bond-stretching mode in the lead–oxygen system. This mode becomes Raman active under the lack of centre of inversion that arises from the off-centred displacement of Pb^{2+} ions. The Pb^{2+} cations can easily form elongated lone pairs if they are linked with B cations of different valence. The atoms may shift from ideal positions due to difference in covalency of the B′–O and B″–O bonds and in such a manner lone pairs oriented along the direction of the shift in the B cations appear. The shift in the position of Pb^{2+} ions, and the orientation of lone pair electrons, depend on the local symmetry. The XRD pattern (figure 1) indicates that the intensity of reflection peaks corresponding to antiparallel off-centred displacement of Pb^{2+} ions gradually decreases with increase in Ba^{2+} concentration and they cease to exist for $x > 0.15$. According to Mihailova *et al* [19], the ratio of intensities of the peaks I_{353}/I_{303} is a measure of the chemical ordering at the B-site. If ordering exists in the B-site, the orientations of lone pairs are correlated and all Pb^{2+} atoms shift in the same direction with respect to O atoms. If the ordering does not exist there is random shifting of the lone pairs and hence atoms. The higher the ratio the greater the ordering and vice versa. The ratio is high for $x = 0$, 0.05 and then decreases, as can be observed from figure 4. The decrease in the chemical ordering should also result in broadening of the A_{1g} phonon mode (near 812 cm^{-1}), which is not observed in our study. Therefore, the decrease in the intensity ratio (I_{353}/I_{303}) of the peaks is attributed to the decrease in the concentration of lone pairs of electrons due to substitution of Ba^{2+} ions and not due to the chemical ordering in the B-site.

The other F_{1u} mode at 420 cm^{-1} began to appear from $x = 0.05$. At room temperature this mode is not seen for PYN. However, for PMW some low intensity modes in the ranges 400–410 and 440–450 cm^{-1} are observed at 10 K [23]. Since PYN and PMW are structurally similar, one can expect modes in the above-mentioned range in the low temperature Raman spectra of PYN. In the present work, with the room temperature data alone for PYN, it is very difficult to reach a conclusion about the presence of the mode around 420 cm^{-1}. Low temperature Raman spectra for some of the compounds in the $(Ba_xPb_{1-x})(Yb_{0.5}Nb_{0.5})O_3$ solid solution series are necessary to underpin more discussion on the characteristics of the mode. However, in relaxor ferroelectric compounds such as PMN, PSN and PST, modes in the range

420–440 cm^{-1} are observed over a wide temperature range [19, 26–28]. Mihailova *et al* [19], on the basis of phonon mode calculations, assigned the modes in the frequency range 420–440 cm^{-1} to the asymmetric O–B–O bending vibration having F_{1u} symmetry arising from rhombohedral structural distortion. In the present $(Ba_xPb_{1-x})(Yb0_{.5}Nb_{0.5})O_3$ solid solution series, the other end of the composition range is $Ba(Yb_{0.5}Nb_{0.5})O_3$. This compound belongs to other Ba^{2+} series of compounds such as $Ba(Y_{0.5}Nb_{0.5})O_3$ and $Ba(Y_{0.5}Ta_{0.5})O_3$. The Raman spectra of these series of compounds do not exhibit any modes around 420 cm^{-1} [29, 30]. Therefore it can be expected that the intensity of this mode may begin to decrease for $x > 0.30$. In Ba^{2+} based complex perovskite compounds, Ba^{2+} ions and B ions occupy the cubo-octahedral and octahedral centres formed by oxygen atoms, whereas in Pb^{2+} based complex perovskite compounds, both Pb^{2+} and B ions exhibit a shift from cubo-octahedral and octahedral centre positions. From the XRD pattern (figure 1), it can be seen that the intensity of the reflections due to off-centred displacement of Pb^{2+} ions decreases with increase in Ba^{2+} and completely vanishes beyond $x = 0.15$, indicating a structural change from orthorhombic to cubic. For cubic $Fm3m$ symmetry, group theoretical analysis predicts only four Raman active modes. However, eight modes are clearly observed in the spectra for the compositions $x = 0.20$–0.30. This indicates the existence of some lower symmetry structure in addition to 1:1 ordering. Choo and Kim [10] attributed the evolution of the hysteresis loop and the broadening and disappearance of the heat capacity anomaly in the $(Ba_xPb_{1-x})(Yb_{0.5}Nb_{0.5})O_3$ solid solution series to the appearance of local polar regions of low symmetry within the non-polar matrix. In the case of PMN, detailed x-ray and neutron diffraction studies indicate, in addition to the average cubic symmetry, the existence of nanometre size polar clusters of local rhombohedral $R3m$ symmetry [31]. The dielectric response of the relaxor ferroelectrics is viewed as the relaxation of these polar clusters over wide temperature and frequency ranges. Recently, nanoscale phase separation has been observed in perovskite type manganites between ferromagnetic metallic and non-ferromagnetic insulating phases, which is very similar to that observed in relaxor ferroelectrics [32, 33]. In the $La_{1-y}Sr_yMnO_3$ solid solution series, the $y = 0.1$ compound is of orthorhombic symmetry whereas the $y = 0.2$ one is of rhombohedral symmetry [34, 35]. The presence of a mode at 420 cm^{-1} in the Raman spectrum in addition to the orthorhombic modes at 30 K for $y = 0.1$ is attributed to the existence of an orthorhombic phase with rhombohedral distortion. The presence of a mode at 420 cm^{-1} for $y = 0.2$ further validates the assignment of this mode to rhombohedral symmetry. Thus the appearance of the mode at 420 cm^{-1} from $x = 0.05$ in the present study can be attributed to the existence of rhombohedral symmetry.

The presence of ordered regions with a particular symmetry allows the appearance of specific Raman modes that are otherwise silent. The presence of the A_{1g} phonon mode (812 cm^{-1}) in all the spectra in our case indicates the existence of chemical ordering in the B-site. This mode is a simple motion of oxygen atoms along the B′–O–B″ axis. This is similar to the breathing-type mode of a free octahedron without involving A or B cations. All the cations are at rest and the cationic mass effect does not come into the picture. The corresponding frequencies depend on the B′–O and B″–O binding forces. The vibrations occur at the highest frequencies of the spectrum since it does not involve the heavy cations. The degree of ordering is estimated from the FWHM of the A_{1g} phonon mode. On the basis of Raman studies on La^{3+} substituted PMN, Jiang *et al* [15, 36] attributed the narrowing of the A_{1g} mode (772 cm^{-1}) from 56 to 38 cm^{-1} to increase in the B-site ordering. However, in the present study we observe only marginal changes in the FWHM of the A_{1g} mode, indicating no effective change in the B-site ordering on substitution of Ba^{2+}. This is further proved by the existence of the F reflection peaks in the XRD (figure 1). The frequency of this mode is expected to decrease with Ba^{2+} substitution, as the ionic radius is greater than that of Pb^{2+} [30].

In the present case, an opposite trend is observed, indicating an increase in the force constant of the B–O bond.

The E_g symmetry mode at 772 cm^{-1} does not involve the motion of cations. This mode is predominantly observed for the compositions $x = 0.25$ and 0.3.

From the earlier discussions it can be inferred that the phonon modes at 55, 520, 772 and 812 cm^{-1} are the modes due to true Raman activity for the space group $Fm3m$. The presence of additional modes at 200, 265 and 420 cm^{-1} indicate the existence of lower symmetry structure, which in the present study is attributed to the local rhombohedral distortion. The increase in the intensity of the lines at 200 and 420 cm^{-1} with increase in Ba^{2+} content indicates an increase in the number of such polar regions with local rhombohedral distortion. Correspondingly, the dielectric response becomes more diffuse and exhibits relaxor behaviour. Even though the dielectric response begins to show relaxor behaviour from $x = 0.1$, the Raman spectra indicate the appearance of rhombohedral distortion from $x = 0.05$. The reason is that the fraction of the cells exhibiting the local distortion might be very much less. Therefore for $x = 0.05$, the dielectric studies could not detect the frequency dispersion of the low fraction polar regions. Since Raman scattering probes the variation within a few unit cells, the local distortion could be detected in the Raman spectra from $x = 0.05$. The electron–phonon coupling due to Pb^{2+} lone pair electrons leads to modes at 303 and 353 cm^{-1}. This explains the presence of nine modes, in contradiction to the four modes possible for $Fm3m$. The modes at 105, 142, 167, 192 and 650 cm^{-1} correspond to orthorhombic symmetry. The modes due to orthorhombic symmetry gradually disappear, which is further evidenced by the disappearance of the reflections corresponding to antiparallel displacement of Pb^{2+} ions. The cubic symmetry with local rhombohedral distortion without any trace of orthorhombic symmetry commences at around $x = 0.2$.

4. Conclusions

The structural variations associated with the substitution of Ba^{2+} in PYN are studied using x-ray diffraction, dielectric and Raman spectroscopic measurements. The x-ray diffraction indicates a gradual decrease in the intensity and disappearance of the reflections corresponding to antiparallel displacement of Pb^{2+} ions, whereas the F reflections remain for the compositions studied. Raman studies indicate the presence of lower local symmetry in addition to 1:1 ordering. The local symmetry is assigned to rhombohedral distortion, which is reflected by the diffuseness observed in the dielectric response. The local distortion commences around $x = 0.05$ and increases with increase in Ba^{2+}, which is evident from the increase in the intensity of the peaks near 200 and 421 cm^{-1}. The commencement of local rhombohedral distortion does not show diffuseness in the dielectric response for $x = 0.05$. This might be due to the distortion being very diluted and cannot be detected with dielectric measurements.

References

[1] Setter N and Cross L E 1980 *J. Appl. Phys.* **51** 4356–60
[2] Chu F, Setter N and Taganstev A K 1993 *J. Appl. Phys.* **74** 5129–34
[3] Viehland D and Li J F 1994 *J. Appl. Phys.* **75** 1705–8
[4] Chu F, Reaney I M and Setter N 1995 *J. Appl. Phys.* **77** 1671–6
[5] Randall C A and Bhalla A S 1990 *Japan. J. Appl. Phys.* **29** 327–33
[6] Randall C A, Bhalla A S, Shrout T R and Cross L E 1990 *J. Mater. Res.* **5** 829–34
[7] Kwon J R, Choo C K K and Choo W K 1991 *Japan. J. Appl. Phys.* **30** 1028–33
[8] Choo W K, Kim H J, Yang H L, Lee J Y, Kwon J R and Chun C H 1993 *Japan. J. Appl. Phys.* **32** 4249–53
[9] Vedantam R R, Subramanian V, Sivasubramanian V and Murthy V R K 2004 *Mater. Sci. Eng.* B **113** 136–42

[10] Choo W K and Kim H Y 1992 *J. Phys.: Condens. Matter* **4** 2309–21
[11] Kim H S and Choo W K 2002 *Ferroelectrics* **269** 147–52
[12] Kim H S, Kim J H, Choo W K and Setter N 2001 *J. Eur. Ceram. Soc.* **21** 1665–8
[13] Husson E, Abello L and Morell A 1990 *Mater. Res. Bull.* **25** 539–45
[14] Ohwa H, Iwata M, Orihara H, Yasuda N and Ishibashi Y 2001 *J. Phys. Soc. Japan* **70** 3149–54
[15] Jiang F, Kojima S, Zhao C and Feng C 2000 *J. Appl. Phys.* **88** 3608–12
[16] Kim B K 2002 *Mater. Sci. Eng.* B **94** 102–5
[17] Setter N and Laulicht I 1987 *Appl. Spectrosc.* **41** 526–8
[18] Bismayer U, Devarajan V and Groves P 1989 *J. Phys.: Condens. Matter* **1** 6977–86
[19] Mihailova B, Bismayer U, Guttler B, Gospodinov M and Konstantinov L 2002 *J. Phys.: Condens. Matter* **14** 1091–105
[20] Baldinozzi G and Sciau Ph 1995 *Acta Crystallogr.* B **51** 668–73
[21] Choo W K, Kim H J, Yang J H, Lim H, Lee J Y, Kwon J R and Chun C H 1993 *Japan. J. Appl. Phys.* **32** 4249–53
[22] Baldinozzi G, Sciau Ph and Bulou A 1996 *J. Phys.: Condens. Matter* **7** 8109–17
[23] Kania A, Jahfel E, Kugel G E, Roleder and Hafid M 1995 *J. Phys.: Condens. Matter* **8** 4441–53
[24] Chen I W, Li P and Wang Y 1996 *J. Phys. Chem. Solids* **57** 1525–36
[25] Burton B P 2000 *J. Phys. Chem. Solids* **61** 327–33
[26] Idink H and White W B 1994 *J. Appl. Phys.* **76** 1789–93
[27] Iwata M, Tomisato N, Orihara H, Ohwa H, Yasuda N and Ishibashi Y 2001 *Ferroelectrics* **261** 83–8
[28] Ohwa H, Iwata M, Yasuda N and Ishibashi Y 1998 *Ferroelectrics* **218** 53–61
[29] Gregora I, Petzelt J, Pokomy J, Vorlicek V, Zikmund Z, Zurmuhlen R and Setter N 1995 *Solid State Commun.* **94** 899–903
[30] Siny I G, Tao R, Katiyar R S, Guo R and Bhalla A S 1998 *J Phys. Chem. Solids* **59** 181–95
[31] de Mathan N, Husson E, Calvarin G, Gavarri J R, Hewat A W and Morell A 1991 *J. Phys.: Condens. Matter* **3** 8159–71
[32] Bibes M, Balcells L, Valencia S, Fontcuberta J, Wojcik M, Jedryka E and Nadolski S 2001 *Phys. Rev. Lett.* **87** 067210
[33] Kimura T, Tomioka Y, Kumai R, Okimoto Y and Tokura Y 1999 *Phys. Rev. Lett.* **83** 3940–3
[34] Granado E, Moreno O, Gracia A, Sanjurjo J A, Rettori C, Torriani I, Oseroff S B, Neumeier J J, McClallan K J, Cheong S W and Tokura Y 1998 *Phys. Rev.* B **58** 11435–40
[35] Bjorrnsson P, Rubhausen M, Backstrom J, Kail M, Eriksson S, Eriksen J and Borjesson L 2000 *Phys. Rev.* B **61** 1193–7
[36] Jiang F, Kojima S, Zhao C and Feng C 2001 *Appl. Phys. Lett.* **79** 3938–40